INTERNATIONAL JOURNAL OF OPTIMIZATION IN CIVIL ENGINEERING
Int. J. Optim. Civil Eng., 2014; 4(3):399-413

A Novel Methodology for Structural Matrix Identification using Wavelet Transform Optimized by Genetic Algorithm

G. Ghodrati Amiri[*, †] and M. Talebi
School of Civil Engineering, Iran University of Science & Technology, Tehran, Iran

ABSTRACT

With the development of the technology and increase of human dependency on structures, healthy structures play an important role in people lives and communications. Hence, structural health monitoring has been attracted strongly in recent decades. Improvement of measuring instruments made signal processing as a powerful tool in structural heath monitoring. Wavelet transform invention causes a great evolution in signal processing. Wavelet transform decomposes a signal into several groups based on scaled and translated basic functions. In this study, a novel methodology based on wavelet transform using complex Morlet wavelet has been introduced for system identification. This process includes a multivariable constrained optimization problem for selecting suitable complex Morlet wavelet. Using selected wavelet, modal parameters and flexibility matrix of structure can be estimated properly. Because of small modal participation of higher mode; using finite number of modes leads to flexibility matrix with acceptable accuracy. Since damages cause change in structural properties, a damage index based on flexibility matrix has been applied and its performance has been investigated in some structures.

Received: 20 April; Accepted: 15 October

KEY WORDS: system identification; matrix updating; signal processing; wavelet transform; genetic algorithm.

1. INTRODUCTION

After 2nd world war, building construction developed widely around the world. However,

[*]Corresponding author: School of Civil Engineering, Iran University of Science & Technology, Tehran, Iran
[†]E-mail address: ghodrati@iust.ac.ir (G. Ghodrati Amiri)

lifetime of human built structure is limited. Dilapidation and different internal and external factors damage and even destruct structures. For this reason, several studies have been conducted to detect structural damage.

For health monitoring of structures, several methods based on structural response to different load conditions has been introduced. These methods are based on that damages cause change in physical properties (mass, stiffness and damping) of structure and thus, change its dynamic characteristic (natural frequency, mode shape, damping ratio, ...). Hence, investigating dynamic parameters of structure can help to find location of damage as well as its severity [1, 2].

The resonance frequency was used widely as a damage index in primary structural health monitoring (SHM) methods which were based on vibration response analysis. Because of low sensitivity of frequency to damage and its changes due to environmental condition, these methods are not reliable [3-5]. Mode shapes and its properties such as mode shape curvature, modal strain energy and dynamic flexibility are properties which substituted for frequency. Since slight damages have little influence on modal parameters in lower modes, accuracy of these methods depends on the number of implemented modes. Large number of mode increase the accuracy of methodology, but it is not economical [6-8].

Improvement of measuring instruments introduced other methods in SHM which directly use vibrational data. These methods are based on signal processing [9-11]. In signal processing, the part of signal which has all of its effects is considered. Generally, signals can be divided into stationary and non-stationary groups. In non-stationary signal, e.g. structural vibration response, signal behavior varies with time. This characteristic of signals should be considered for choosing the appropriate signal processing method. Based on signal type, several signal processing methods such as Fourier Transform (FT), Wavelet Transform (WT) and Hilbert Transform (HT) has been presented [12-14].

In the remaining of this paper, first a brief description of WT is introduced. After that a methodology for finding natural frequencies and mode shapes using free vibration acceleration response of structure based on WT is presented. Using obtained modal parameter and given mass, flexibility matrix of structure can be determined. Then, a Damage Index (ID), based on flexibility matrix, is implemented in order to control structural state. The performance of the proposed methodology is checked with obtained data from numerical model of two laboratory models.

2. WAVELET TRANSFORM

Wavelet Transform (WT) invention causes a great evolution in signal processing. WT is linear time-frequency method which expresses signal using a group of scaled and translated signals. Wavelet, $\psi(t)$, is a mother wave which is centered at specific time and has a very short duration and finite energy [15].

$$\int_{-\infty}^{+\infty} \psi(t)dt = 0 \tag{1}$$

In a wavelet where $t=0$ is supposed as center of time, center frequency (η), time domain (σ_t^2) and frequency domain (σ_ω^2) variance are obtained using Eq. (2) to Eq. (4) [15].

$$\eta = \frac{1}{2\pi E_\psi}\int_0^\infty \omega\left|\hat{\psi}(\omega)\right|^2 d\omega \tag{2}$$

$$\sigma_t^2 = \frac{1}{E_\psi}\int_{-\infty}^{+\infty} t^2\left|\psi(t)\right|^2 dt \tag{1}$$

$$\sigma_\omega^2 = \frac{1}{2\pi E_\psi}\int_{-\infty}^{+\infty} (\omega-\eta)^2\left|\hat{\psi}(\omega)\right|^2 d\omega \tag{2}$$

Wavelet can be real or imaginary. In study of vibrational behavior, imaginary wavelets are more effective because they can determine phase and amplitude information of signal. However, real wavelets are appropriate for peak isolation and determining non-uniformity.

2.1 Continuous wavelet transform (CWT)

A wavelet family, $\psi_{u,s}(t)$, is a group of basic functions which obtained from scaled and translated wavelet.

$$\psi_{u,s}(t) = \frac{1}{\sqrt{s}}\psi\left(\frac{t-u}{s}\right) \tag{5}$$

Where *u* and *s* are translation and scale parameter, respectively. For each pair of *u* and *s*, $\psi_{u,s}(t)$ is a child wavelet. Where *s* increases, the wavelet dilates in time domain and its amplitude decreases. Also, increase of scale parameter leads to decrease of the center frequency and frequency bandwidth.

CWT of $f(t)$ expresses the similarity between signal and $\psi_{u,s}(t)$ wavelet family for several values of *u* and *s* and can be calculated using Eq. (6) [15]:

$$wf(u,s) = \int_{-\infty}^{+\infty} f(t)\frac{1}{\sqrt{s}}\psi^*\left(\frac{t-u}{s}\right)dt \tag{6}$$

Where *, denotes complex conjugate. $wf(u,s)$ are coefficients corresponding to time *u* and scale *s*. Properties of CWT is dependent on mother wavelet. Using Eq. (7), $f(t)$ can be reconstructed based on wavelet coefficient [15].

$$f(t) = \frac{1}{C_\psi}\int_{-\infty}^{+\infty}\int_{-\infty}^{+\infty} wf(u,s)\frac{1}{\sqrt{s}}\psi\left(\frac{t-u}{s}\right)du\frac{ds}{s^2} \tag{7}$$

$$C_\psi = \int_{-\infty}^{+\infty} \frac{|\hat{\psi}(\omega)|}{\omega} d\omega < +\infty \tag{3}$$

Time-Frequency Resolution of WT is function of Heisenberg rectangle with σ_t and σ_ω of mother wavelet. Scaled and translated wavelet has *u* center time and η/s frequency center and its time and frequency variance are $s\sigma_t^2$ and σ_ω^2/s, respectively. Therefore, resolution of WT changes with *s*, but the area of rectangle is the same [15].

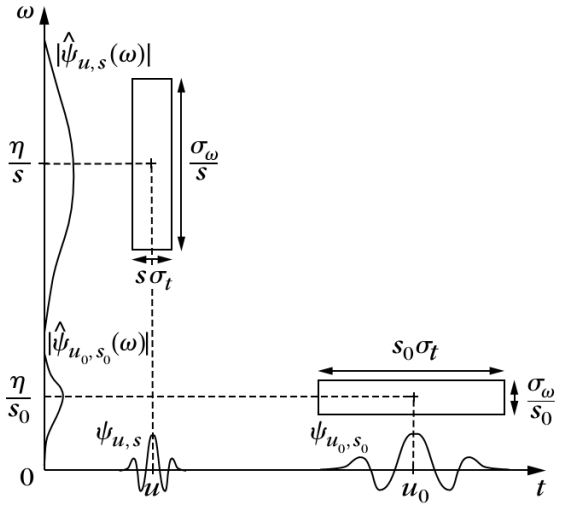

Figure 1. Heisenberg rectangle of $\psi_{u,s}$ for different scale [15]

Frequency resolution has direct relation with scale parameter, while time resolution decreases with scale parameter growth. Therefore, high frequency signals should be evaluated with small scale parameters whereas higher scales should be used for low frequency signals.

2.2 Analytical Wavelet Transform

For assessment the time evolution of a signal, analytical wavelet which can separate phase and amplitude information of a signal must be used. f_a is an analytical function if its FT for negative frequency is zero. In analytical wavelet transform, an analytical wavelet, which is equal to a sine wave multiplied by a window, is used. This transform is like Windowed Fourier Transform (WFT) with varied scale [15].

$$Wf(u,s) = \langle f, \psi_{u,s} \rangle = \langle f, g_{u,s,\xi} \rangle e^{i\xi u} \tag{9}$$

Eq. (9) expresses analytical wavelet transform in which $\langle , \rangle$ is inner product.

Based on [16], for $x(t) = A(t)\cos(\omega t)$ with $Z(t) = A(t)e^{i\omega t}$ analytical form, its analytical

wavelet transform is calculated using Eq. (10).

$$Wf(u,s)=\left\langle x(t),\psi_{u,s}(t)\right\rangle=\frac{1}{2}\left\langle x_a(t),\psi_{u,s}(t)\right\rangle=\frac{1}{2}\int_{-\infty}^{\infty}A(t)e^{i\omega t}\psi_{u,s}^{*}(t)dt \tag{10}$$

Using Taylor series of $A(t)$ at $t=u$ and neglecting of the terms with order higher than1, because of negligible amount of $A'(t)$ around $t=u$; the Eq. (10) is simplified into Eq. (11) [16].

$$Wf(u,s)=\frac{1}{2}\int_{-\infty}^{\infty}(A(u)+o(A'(u))e^{i\omega t}\psi_{u,s}^{*}(t)dt=\frac{\sqrt{s}}{2}A(u)\hat{g}(s\omega_0-\eta)e^{i\omega_0 u} \tag{11}$$

Generalized form of Eq. (11), for WT of $x(t)=A(t)\cos(\varphi(t))$ is obtained using Eq. (12).

$$Wf(u,s)=\frac{\sqrt{s}}{2}A(u)\hat{g}(s\varphi'(u)-\eta)e^{i\varphi(u)} \tag{12}$$

3. SYSTEM IDENTIFICATION

3.1 Frequency and damping ratio recognition

Eq. (13) gives free vibration response of a n DOF system [17]:

$$\begin{aligned}x(t)&=\sum_{i=1}^{n}A_i e^{-2\pi\zeta_i f_i t}\cos(2\pi f_d t+\theta_i)\\ \ddot{x}(t)&=\sum_{i=1}^{n}A_i' e^{-2\pi\zeta_i f_i t}\cos(2\pi f_d t+\theta_i)\end{aligned} \tag{13}$$

Where $x(t)$ and $\ddot{x}(t)$ are displacement and acceleration free vibration response of structure, respectively. In this equation, A_i or A_i' and θ_i denotes amplitude and phase angle of motion, respectively. f_i and $f_{di}=f_i\sqrt{1-\xi_i^2}$ are un-damped and damped natural frequency and ξ is damping ratio. Mode number is indicated by *i*.

Acceleration response is more applicable in signal processing because of its higher frequency content than displacement. By using complex Morlet wavelet, based on previous sections, WT of acceleration response is given by Eq. (14).

$$Wf(u,s)=\frac{\sqrt{s}}{2}\sum_{i=1}^{n}A_i' e^{-2\pi\zeta_i f_i u}e^{-\pi^2 f_b(sf_i-f_c)^2}e^{j(2\pi f_{d_i}s+\theta_i)} \tag{14}$$

Complex Morlet wavelet, with f_c center frequency and f_b frequency bandwidth, is one of the most common wavelets in signal processing. If $\sqrt{f_b}\, f_c \geq \sqrt{2}$, the simplified relation of Morlet wavelet in time and frequency domain is expressed using Eq. (15) and Eq. (16), respectively [13].

$$\psi(t) = \frac{1}{\sqrt{\pi f_b}} e^{j2\pi f_c t} e^{-t^2/f_b} \tag{15}$$

$$\psi(af) = e^{-\pi^2 f_b (sf - f_c)^2} \tag{4}$$

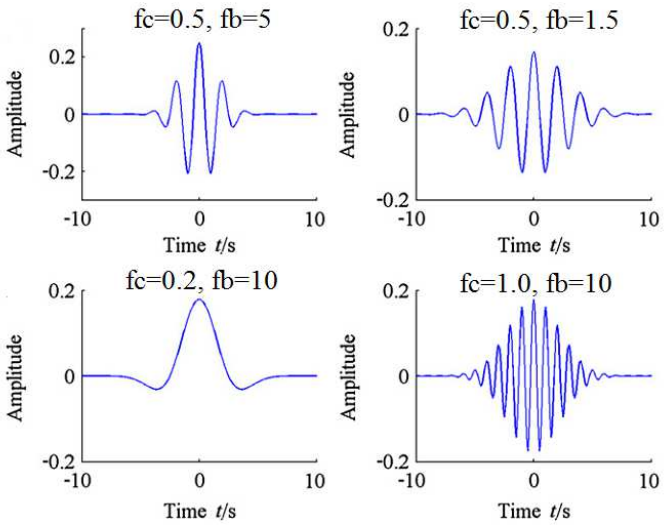

Figure 2. Morlet wavelet for different f_b and f_c [18]

Fig. 2 shows that frequency resolution has direct and indirect relation with f_b and f_c, respectively. For $s_i = f_c / f_i$, Eq. (17) gives σ_{ti} and $\sigma_{\omega i}$.

$$\sigma_{ti} = s_i \sigma_{t\psi} = \frac{f_c}{f_i} \frac{\sqrt{f_b}}{2}, \sigma_{\omega i} = \frac{1}{s_i} \sigma_{\omega\psi} = \frac{f_i}{f_c} \frac{1}{\sqrt{f_b}} \tag{17}$$

Based on Heisenberg principle ($\sigma_t \sigma_\omega \geq 1/2$) and Eq. (17), f_b, f_c should be chosen such that appropriate time and frequency resolutions are obtained. A solution for this selection is finding a pair which minimizes the modified Shannon entropy. Eq. (18) presents modified Shannon entropy [18].

$$E^k(f_b) = -\sum_{i=1}^{M} d_i^k \log(d_i^k) \ , \ \sum_{i=1}^{M} d_i^k = 1 \ , \ f_c = k \in [J, K] \tag{18}$$

$$d_i^k(f_b) = \frac{\left|Wf^k(u,s_i)\right|}{\sum_{j=1}^{M} Wf^k(u,s_j)} \tag{5}$$

It is observed that $s = s_i = f_c / f_i$ maximizes $e^{-\pi^2 f_b (sf_i - f_c)^2}$. In this situation, the corresponding mode of f_i has the most participation in wavelet coefficients.

$$Wf(u,s_i) = \frac{\sqrt{s_i}}{2} A_i' e^{-2\pi\zeta_i f_i u} e^{j(2\pi f_{d_i} u + \theta_i)} \tag{20}$$

Rewriting Eq. (20) and substituting *t* for *u* leads to Eq. (21).

$$Wf(t,s_i) = \frac{\sqrt{s_i}}{2} A_i' e^{-2\pi\zeta_i f_i t} e^{j(2\pi f_{d_i} t + \theta_i)} = B_i(t) e^{j(\varphi_i(t))} \tag{21}$$

By applying exponential logarithm and derivative, separately, to the amplitude and phase of wavelet coefficients and combining obtained equations, natural frequencies and damping ratios are achieved [13].

$$\ln(B_i(t)) = -2\pi\zeta_i f_i t + \ln(\frac{\sqrt{s_i}}{2} A_i') \rightarrow \frac{d(\ln(B_i(t)))}{dt} = -2\pi\zeta_i f_i \tag{22}$$

$$\frac{d(\varphi_i(t))}{dt} = 2\pi f_{d_i} = 2\pi f_i \sqrt{1-\xi_i^2} \tag{6}$$

$$f_i = \sqrt{(\frac{d\ln(B_i(t))}{dt})^2 + (\frac{d\phi_i(t)}{dt})^2} \Big/ 2\pi \tag{7}$$

$$\xi_i = (\frac{d\ln(B_i(t))}{dt}) \Big/ 2\pi f_i \tag{8}$$

For decomposing two closely spaced frequency component, f_i, f_{i+1}, assuming $f_{i,i+1} = (f_i + f_{i+1})/2$ and $\Delta f_{i,i+1} = f_{i+1} - f_i$, Eq. (27) can be obtained from Eq. (17).

$$\Delta f_{i,i+1} \geq (2\alpha) \frac{f_{i,i+1}}{\sqrt{f_b f_c}} \tag{26}$$

$$\sqrt{f_b} f_c \geq (2\alpha) \frac{f_{i,i+1}}{\Delta f_{i,i+1}} \tag{9}$$

In Eq. (26) and Eq. (27), α is a parameter which defines the allowable overlap of two

adjacent Gaussian windows of Morlet wavelet. The possibility of complete modal separation is in direct relation with α. Previous studies show that $\alpha = 2$ is an optimum parameter [13].

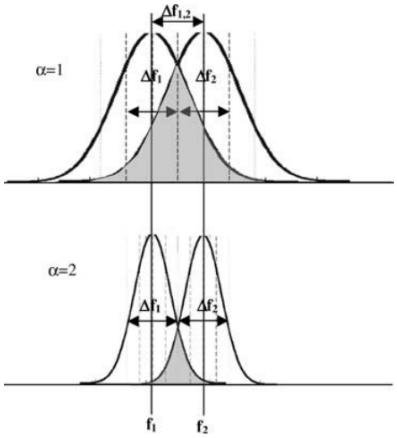

Figure 3. Schematic demonstration of effect of α on mode seperation [19]

The other factor which affects wavelet coefficients is end-effect. Fig. 4 shows that despite wavelet focusing at a specific time and representing the frequency content of signal in its neighborhood, at both beginning and end of signal, the time window may extend to out of signal domain. In order to eliminate the end-effect, a specific length of signal, ΔT_i, should be neglected [13, 19].

$$\Delta T_i = \beta \delta_{ti} = \beta \frac{f_c}{f_i} \frac{\sqrt{f_b}}{2} \tag{28}$$

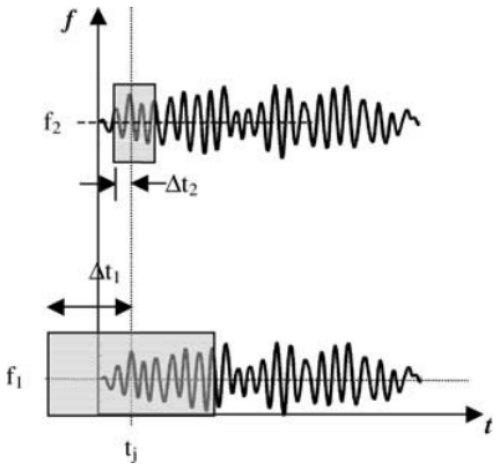

Figure 4. Schematic demonstration of end-effect [19]

Researches show that for $\beta \geq 4$, the end-effects are negligible. If ΔT_i is defined such that $\Delta T_i \leq \gamma T$, the Eq.(29) should be satisfied. In this equation T is the length of signal [13].

$$\sqrt{f_b f_c} \leq (\frac{2\gamma}{\beta}) T f_i \tag{29}$$

As a result, finding f_b and f_c is constrained optimization problem in which modified Shannon entropy should be minimized such that f_b and f_c situate in the following range.

$$(2\alpha)\frac{f_{i,i+1}}{\Delta f_{i+1}} \leq \sqrt{f_b f_c} \leq (\frac{2\gamma}{\beta}) T f_i \tag{30}$$

Among computational intelligent techniques like Genetic Algorithm (GA), Particle Swarm Optimization (PSO), Simulated Annealing (SA) and Neural Network (NN), GA is a powerful tool for solving constrained multi variable problems [20].

GA is a population based probabilistic technique for solving complex problems through the application of the principles of evolutionary biology which is similar to Darwin's theory. In this method, participation of a member is presented by a fitness value. New and more evolutionary-fit individual solutions are produced during a cycle of generations. This process continues until reaching optimum solution [21]. GA includes following steps:

Initialization: At first, a population of individual is selected randomly.

Crossover: Genetic information of the population is combined by cutting and exchanging their chromosomes. This operation increases the potential for joining successful members.

Mutation: In this step, structure of some individual changes randomly. This operation prevents the population from trapping GA in local solutions.

Selection: For every generation, a selection of the proportion of the existing population is chosen to breed a new population

Termination: Previous steps are repeated until stopping criteria is satisfied.

3.2 Mode shapes determination

k-th mode shape can be obtained from WT of recorded signals in all DOFs for k-th frequency. To achieve this purpose, j-th component of k-th complex mode shape, $\varphi_{kj} = r_{kj} + s_{kj} i$, is calculated using Eq.(31) by selecting a reference sensor, r [22, 23].

$$\varphi_{kj} = \frac{Wf_j(u, s_k)}{Wf_r(u, s_k)} \tag{31}$$

Where $Wf_j(u, s_k)$ and $Wf_r(u, s_k)$ are wavelet coefficients of j-th and r-th DOF, respectively. Since φ_{kj} is not constant in signal duration, actual and estimated real mode shapes are different. Eq. (32), presents an optimum estimation of k-th mode in order to decrease this mismatch.

$$r_{kj} = \frac{\sum_{i=1}^{n} q_k(u_i, s_j) q_r(u_i, s_j)}{\sum_{i=1}^{n} q_r^2(u_i, s_j)}, s_{kj} = \frac{\sum_{i=1}^{n} q_k(u_i, s_j) p_r(u_i, s_j)}{\sum_{i=1}^{n} q_r^2(u_i, s_j)} \tag{32}$$

Where $p_k(u_i, s_j)$ and $p_k(u_i, s_j)$ are real and imaginary part of wavelet coefficients and *n* is the signal duration [22, 23].

3.3 Flexibility matrix estimation

Each column of flexibility matrix is the displacement of all DOF due to unit load on the corresponding DOF of column. Therefore, the flexibility matrix can be obtained by imposing unit load on each DOF and measuring the displacement of all DOFs [24]. This process would be difficult and impossible for complex structures which include high DOF.

If mode shapes are normalized such that $\phi^T M \phi = I$, flexibility matrix of structure can be obtained using Eq.(33) [25].

$$F = \phi \Lambda^{-1} \phi^T = \sum_{i=1}^{n} \frac{1}{\omega_i^2} \phi_i \phi_i^T \tag{33}$$

Where *F* is flexibility matrix, $\phi = [\phi_1, \phi_2, \ldots, \phi_n]$ is normalized mode shape matrix, ϕ_i is i-th mass normalized mod shape, Λ is diagonal matrix of Eigen values and *n* is the DOF number. Because of inverse relation between flexibility matrix and mode order, only limited number of modes leads to a matrix with acceptable accuracy. So, with frequencies and modes shapes which were obtained from previous sections, the flexibility matrix can be calculated easily.

3.4 Structural assessment using flexibility matrix

Structural damage causes change in flexibility matrix. Thus, comparing flexibility matrix with its primary condition and health state would be an appropriate approach for recognition of location and severity of damage. In this study, a Damage Index (DI) based on flexibility matrix is implemented.

$$DI_i = 100 \times \left(\sum_{j=1}^{n} \left[(f_{ij}^{H} - f_{ij}^{D}) / f_{ij}^{H} \right]^{0.5} \right)^2 \tag{34}$$

Where DI_i is damage index in i-th DOF and f_{ij}^{H} and f_{ij}^{D} are i-th row and j-th column of flexibility matrix in health and damage state, respectively.

4. VERIFICATION OF PROPOSED METHODOLOGY

For verification of proposed method, numerical model of two laboratory model has been investigated. The first one (Fig. 5) is a 3-DOF, two dimensional laboratory model [26]. This model is a 3-story moment frame which presents a building with one-eighth scale. In this model 10mm×10mm and 12mm×12mm steel boxes are used for beams and columns and each story is considered as a 10-kg mass. Fig. 6 shows three first mode shapes of this model. For data acquisition, the acceleration response of the model to an initial displacement has been recorded. Two structural damage scenarios have been considered for this model. The first scenario includes 20% stiffness reduction in the middle 10cm of third story columns and the second one is 20% stiffness reduction in the middle 10cm of first story columns.

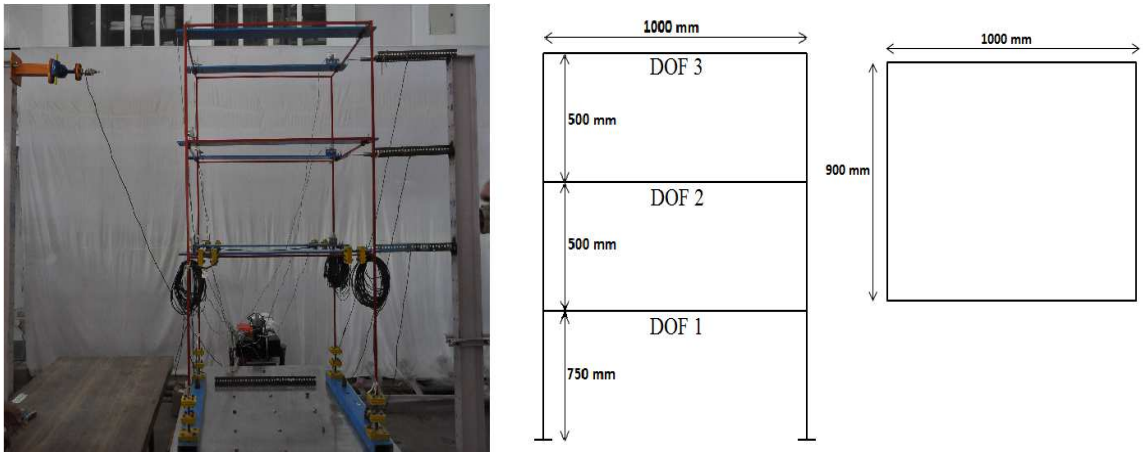

Figure 5. 3-DOF Laboratory Model

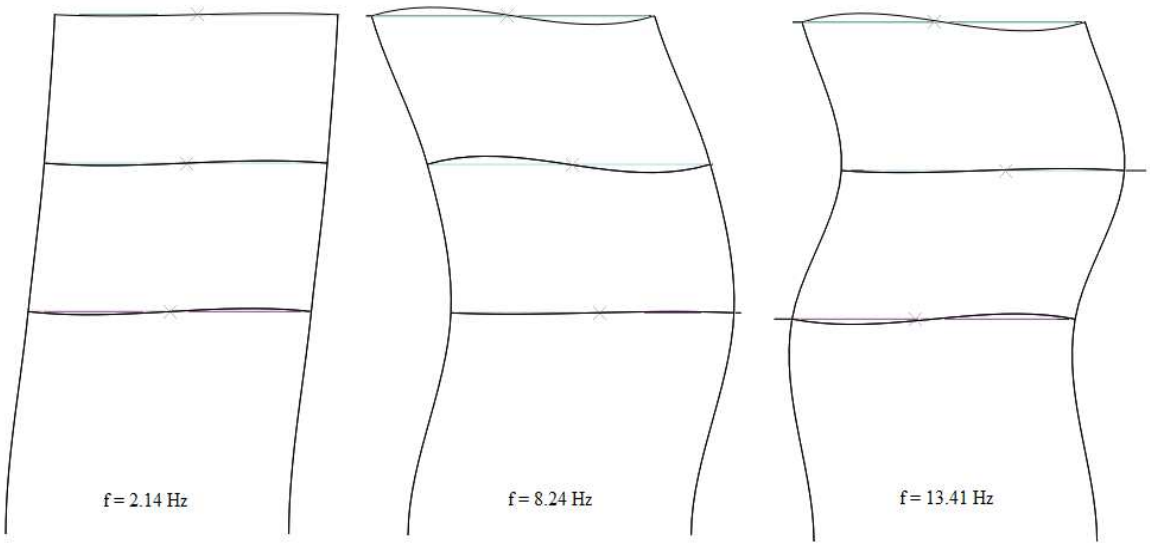

Figure 6. Three first mode shape of 3-DOF model

Table 1: Natural frequencies of 3-DOF models in Hz

	Laboratory (Health)	Numerical (Health)	Estimated (Health)	Estimated (1st scenario)	Estimated (1st scenario)
1st mode	2.14	2.31	2.318	2.328	2.35
2nd mode	8.24	8.11	8.059	8.057	8.045
3rd mode	13.41	14.73	13.495	12.896	13.061

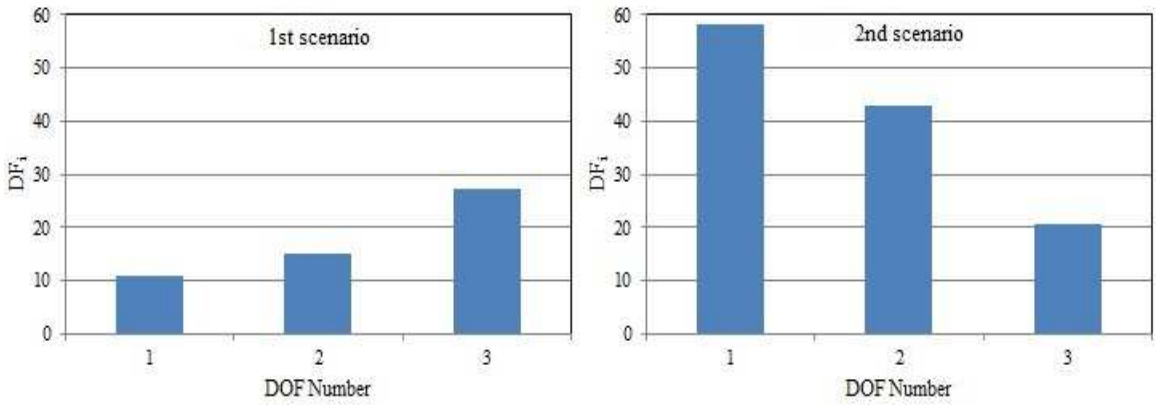

Figure 7. DI in different DOFs of 3-DOF model

The second considered model is a laboratory steel bridge benchmark (Fig. 8) [27, 28]. Deck of this model includes two 18-ft longitudinal and seven 3-ft transvers beam which are made from S3x5.7 connected together with rigid connection. The deck is supported with six 3.5ft W12x26 columns. The connections between deck and columns are hinge. Fig. 9 shows three first modes of benchmark. Acceleration response of the model to a random vertical vibration has been recorded in location which is showed in Fig. 10. It should be noted that the mass of bridge is considered to be concentrated at sensor locations. Releasing the rotational DOF of S11 and S22 has been considered as the first and second structural damage scenario, respectively.

Figure 8. Steel bridge benchmark [28]

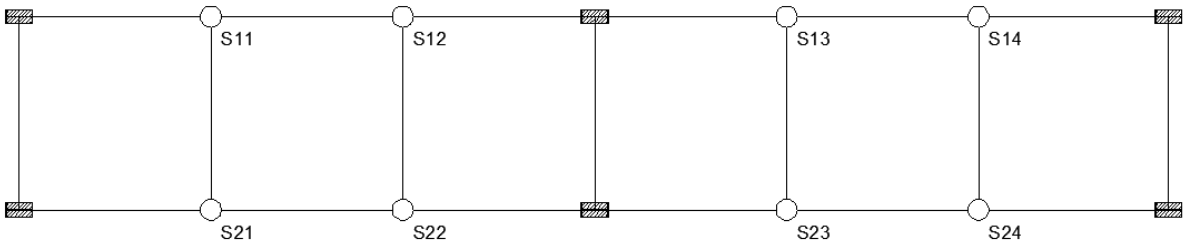

Figure 9. Location of sensors and DOFs

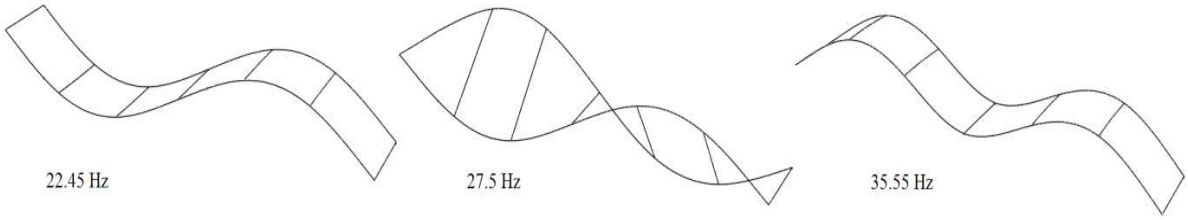

Figure 10. Three fisrt mode shapes of bridge benchmark

Table 2: Natural frequencies bridge benchmark in Hz

	Laboratory (Health)	Numerical (Health)	Estimated (Health)	Estimated (1st scenario)	Estimated (1st scenario)
1st mode	22.37	22.45	23.61	23.61	23.61
2nd mode	27.01	27.5	26.95	26.93	26.93
3rd mode	33.38	33.55	34.66	34.65	34.65

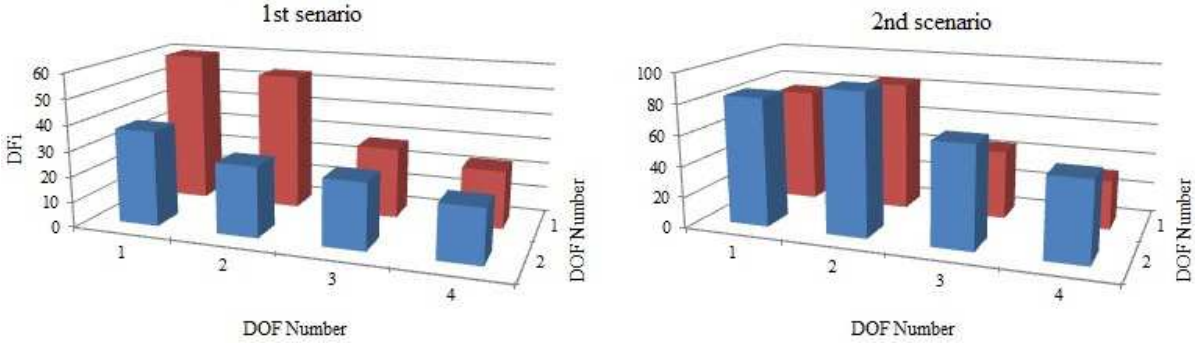

Figure 11. DI in different DOFs of bridge benchmark

5. CONCLUSION

In this paper, a methodology, based on analytical wavelet transform using complex Morlet wavelet has been introduced for determining natural frequencies, mode shapes and flexibility matrix of structure. As mentioned before, Morlet wavelet is a time domain function with two unknown parameters (f_b, f_c). Selection of these two parameters is a

constrained optimization problem. Studies show that if $0 < f_c \leq 1$, more acceptable results can be obtained. In this study, GA has been applied for finding f_b, f_c and it is observed that by considering third DOF as references sensor, (81.34, 1) would be optimum answer in 3-DOF model. Also, (1651.37, 0.99) would be optimum answer in bridge benchmark if S12 is selected as references sensor.

Tables 1 and 2 show experimental, numerical and estimated values of natural frequencies in 3-DOF model and bridge benchmark, respectively. The results show the acceptable level of accuracy in frequency estimation. Also the results show that minor damages have little effect on lower natural frequency modes and these changes give no information about the location of damage.

Figs. 7 and 11 indicate the sensitivity of proposed damage index to location and severity of damage. Proposed DI increases with increase of damage severity.

For future studies, investigating the effects of references location, type and location of imposed loads and studying other kinds of structures and scenarios are suggested.

REFERENCES

1. Doebling SW, et al. *Damage Identification and Health Monitoring of Structural and Mechanical Systems from Changes in Their Vibration Characteristics: A Literature Review*, 1996, Los Alamos, National Laboratory.
2. Sohn H, et al. *A Review of Structural Health Monitoring Literature: 1996–2001*, 2004, Los Alamos, National Labratory.
3. Chi FC. *Assessment of the Structural Integrity of Timber Bridge Using Dynamic Approach*, University of Technology,Syndny, 2007.
4. Turner JD, Pretlove AJ. A study of the spectrum of traffic-induced bridge vibration, *J Sound Vib* 1989; **122**: 31-42.
5. Dackerman U. *Vibration Based Damage Identification Method for Civil Structures Using Artificial Neural Network*, University of Technology, Sydny, 2010.
6. Pandey AK, Biswas M, Samman MM. Damage detection from changes in curvature mode shapes, *J Sound Vib* 1991; **145**: 321-32.
7. Stubbs N, Kim JT, Topple K. An effective and robust algorithm for damage localization in offshore platforms, *ASCE 10th Structural Congress* 1994, San Antonio, Texas.
8. Dossing O. *Structural Testing-Part2: Modal Analysis, in Bruel and Kjaer* 1998, Naerum, Denmark.
9. Ni YQ, Zhou XT, Ko JM. Experimental investigation of seisimic damage identification using pca-compressed frequency response functions and neural network, *J Sound Vib* 2006; **290**: 242-63.
10. Limengoli MP. Frequency response function interpolation for damage detection under changing environment, *Mech Syst Signal Process* 2010; **24**: 2898-2913.
11. Santos JVAD, et al. Structural damage identification in laminated structures using frf data, *J Sound Vib* 2006; **290**: 242-63.
12. Xu YL, SW Chen, RC Zhang. Modal identification of di wang building under typhoon york using hilbert-huang transform method, *Struct Des Tall Spec* 2003; **12**: 21-47.

13. Yan BF, Miyamoto A, Bruhwiler E. Wavelet transform-based modal parameter identification considering uncertainty, *J Sound Vib* 2006; **291**: 285-301.
14. Zhu XQ, Law SS. Wavelet-based crack identification of bridge beam from operational deflection time history, *J Solid Struct* 2006; **43**: 2299-2317.
15. Mallat S. *A Wavelet Tour of Signal Processing, The Sparse way*, Academic Press, 2009.
16. Lardies J, Gouttebroze S. Identification of modal parameters using the wavelet transform, *J Mech Sci* 2002; **44** 2263-83.
17. Chopra AK. *Dynamic of Structures:Theory and Applications to Earthquake Engineering*, Prentice Hall, 2012.
18. Jiang Y, et al. Feature extraction method of wind turbine based on adaptive morlet wavelet and SVD, *J Renew Energ* 2011; **46**: 2146-53.
19. Kijewski T, Kareem A. Wavelet transform for system identification in civil engineering, *Comput Aided Civ Infrastruct Eng* 2003; **18**: 339-55.
20. Gokdag H, Kopmaz O. A new damage detection approach for beam-type structures based on the combination of continuous and discrete wavelet transforms, *J Sound Vib* 2009; **324**: 1158-80.
21. Marwala T. *Finite-element-model Updating Using Computional Intelligence Techniques*, Springer, 2010.
22. Meoa M, et al. Measurements of dynamic properties of a medium span suspension bridge by using the wavelet transforms, *Mech Syst Signal Process* 2006; **20**: 1112-33.
23. Piombo BAD, et al. Modelling and identification of the dynamic response of a supported bridge, *Mech Syst Signal Process* 2000; **14**: 75-89.
24. Kassimali A. *Matrix Analysis of Structures*, Cengage Learning, 2010.
25. Pandey AK, Biswas M. Damage detection in structures using changes in flexibility, *J Sound Vib* 1994; **169**: 3-17.
26. Chugh P, et al. *Small Scale Modeling and Testing of a 3-Story Steel Moment Frame Building - with/Without Base Isolation*, Indian Institute of Technology, Kanpur, 2011.
27. Catbas N, Caicedo JM, Dyke SJ. *Benchmark Problem on Structural Health Monitoring of Highway Bridges*, Structural health Monitoring of Highway Bridges (Phase I) – Long Abstract, 2005.
28. Gul M. *Investigation of Damage Detection Methodologies for Structural Health Monitoring*, Department of Civil Environmental and Construction Engineering, University of Central Florida, 2009.